Subcarrier Assignment and Power Allocation for Device-to-Device Video Transmission in Rayleigh Fading Channels

Peizhi Wu, *Student Member, IEEE*, Pamela C. Cosman, *Fellow, IEEE*, and Laurence B. Milstein, *Fellow, IEEE*

***Abstract*— Subcarrier assignment and power allocation for device-to-device (D2D) video transmission using a filter bank multicarrier waveform in a Rayleigh fading environment are investigated. We analyze the co-channel interference between D2D pairs, and propose a cross-layer algorithm with a subcarrier assignment outer loop and a power allocation inner loop, which aims to optimize the overall video quality. Unlike the non-convexity in physical layer power allocation for maximizing the total throughput, the cross-layer power allocation problem is convex under certain conditions, so a high quality solution for power allocation can be efficiently found. Simulation results demonstrate a higher overall video quality by the proposed cross-layer algorithm compared with baseline algorithms.**

***Index Terms*— Device-to-device communication, multimedia communication, radio spectrum management, cochannel interference.**

I. Introduction

DEVICE-TO-DEVICE (D2D) communication [1] allows direct video delivery between cellular users in close proximity to offload data traffic from the base station (BS). A frequency band can be reused by multiple D2D pairs to improve the spectral efficiency, but the frequency reuse also introduces co-channel interference (CCI) between D2D pairs. In order to improve the overall video quality of a D2D video transmission system with multicarrier waveforms, it is essential to properly assign subcarriers to D2D pairs, and allocate their transmission power.

Centralized resource allocation for D2D systems based on physical layer information was investigated in [2]–[5]. These aimed to maximize the weighted sum rate based on the capacity of the additive white Gaussian noise (AWGN) channel. A practical wireless channel usually experiences fading, so this AWGN model is only applicable when the BS, which is usually the resource allocator, is able to collect the instantaneous channel state information (CSI) in a timely manner. We are concerned with situations in which the base station only knows average CSI and not instantaneous CSI. This might arise for some users because the coherence time is small, or because there are too many users (for example, large crowds in an airport or amusement park). In either case, the overhead for transmitting instantaneous CSI is burdensome. Average CSI is known at the BS either by letting D2D receivers report the average channel gains to the BS, or letting the BS estimate the average channel gains, which includes path loss and shadowing, according to the location information of D2D users. Simple D2D resource allocation algorithms based on average CSI, such as interference avoidance [6], were also investigated in the literature.

The centralized resource allocation problems based on physical layer information considered in [2]–[5] were non-convex, so only heuristic algorithms were proposed. A broader class of these physical layer optimization problems was investigated in [7] as a dynamic spectrum management (DSM) problem, and was shown to be non-convex. The convexity of several extensions for the DSM problem was investigated in [8]. Among these extensions discussed in [8], for the case of multiple users and a single subcarrier, the minimization of a harmonic utility function, which took the capacity of AWGN channel as the argument, was shown to be convex.

Cross-layer resource allocation for cellular video transmission has been investigated in [9]–[13]. In [9], an iterative resource allocation algorithm for video transmission on cellular uplinks was proposed, where every subcarrier was only assigned to a single user. Literature on resource allocation for D2D video delivery included optimization for energy efficiency subject to a QoS constraint [10], and for a utility function that was jointly determined by the throughput and transmission power [11]. A heuristic algorithm to optimize overall video quality of D2D transmission using instantaneous CSI in a quasi-static environment was proposed in [12] and [13]. For discrete bit loading using instantaneous CSI, the transmission power takes on discrete values, so the optimization problem is discrete [12], [13], while in this paper, the D2D pairs are assumed to be able to update the alphabet size according to the instantaneous channel gains under fading, so the transmission power can be chosen from a continuous range, and hence the optimization problem for power allocation based on average channel gain is continuous.

Manuscript received October 8, 2016; revised April 15, 2017 and June 5, 2017; accepted June 6, 2017. Date of publication June 23, 2017; date of current version September 8, 2017. This work was supported by the Army Research Office under Grant W911NF-14-1-0340. The associate editor coordinating the review of this paper and approving it for publication was A. Abrardo. *(Corresponding author: Peizhi Wu.)*

P. Wu was with the Department of Electrical and Computer Engineering, University of California at San Diego, La Jolla, CA 92093 USA. He is now with Qualcomm Tech. Inc., San Diego, CA 92121 USA (e-mail: peizhiw@qti.qualcomm.com).

P. C. Cosman and L. B. Milstein are with the Department of Electrical and Computer Engineering, University of California at San Diego, La Jolla, CA 92093 USA (e-mail: pcosman@ucsd.edu; milstein@ece.ucsd.edu).

Color versions of one or more of the figures in this paper are available online at http://ieeexplore.ieee.org.

Digital Object Identifier 10.1109/TWC.2017.2717823

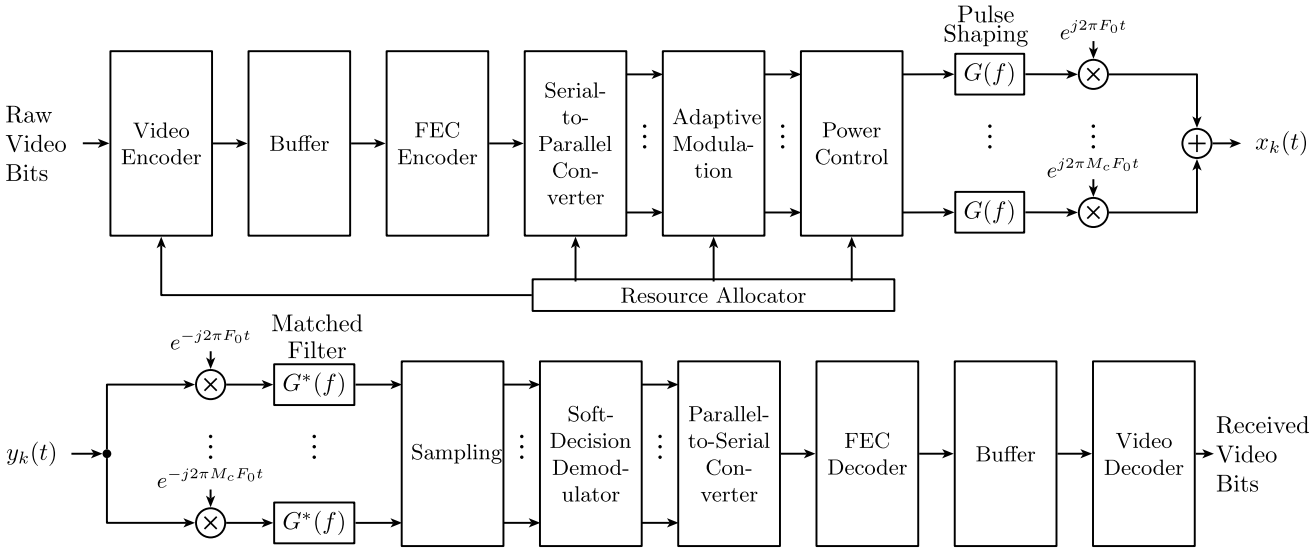

Fig. 1. Block diagram of the transceiver for FMT.

As far as we know, centralized resource allocation for the overall video quality of D2D communication based on the average channel gain and video rate distortion information has not been addressed in the literature.

The novelty of this paper is as follows: 1) Unlike most past work on resource allocation for D2D systems, we propose a cross-layer algorithm to optimize overall video quality rather than physical layer metrics, and have observed considerable improvement on video quality using our proposed cross-layer algorithm; 2) We derived a necessary condition under which the power allocation algorithm for D2D video transmission is convex, which is that the signal-to-interference-and-noise ratio (SINR) of each D2D user must exceed a threshold, as described in Section III.B.

This paper is organized as follows. Section II is the system model. Section III describes the proposed subcarrier assignment and power allocation algorithm, and shows the condition under which the cross-layer power allocation problem is convex. In Section IV, baseline algorithms are presented. Section V presents the simulation results and discussion. Section VI contains the conclusion.

II. System Model

We consider a D2D video transmission system served by a BS. There are K pairs of D2D users in the cell. Each D2D pair consists of a transmitter and a receiver, with a D2D link from the transmitter to the receiver. The system allocates a total frequency band of W (Hz), which is equally divided into M_c subcarriers, exclusively to these D2D pairs [14].

A. Transceiver Architecture

The block diagram of the transceiver is shown in Fig. 1. The transceiver has a multicarrier architecture, where the symbol rate is $1/T_0$ and the frequency spacing of subcarriers is $F_0 = W/M_c$. The complex envelope of the lowpass equivalent signal for the i-th D2D transmitter is given by

$$x_i(t) = \sum_{n=1}^{M_c} \sum_{s} X_{i,n}[s]\, g(t - sT_0)\, e^{j2\pi nF_0 t}, \tag{1}$$

where $g(t)$ is the transmitted pulse, whose energy is normalized to unity, i.e., $\int_{-\infty}^{\infty} |g(t)|^2 = 1$. The FEC protected video bit sequences are mapped to data symbols, where the s-th modulated symbol on the n-th subcarrier of the i-th transmitter is denoted by $X_{i,n}[s]$. The data symbols $\{X_{i,n}[s]\}$ are complex and modulated by square QAM, i.e., $X_{i,n}[s] = X^I_{i,n}[s] + jX^Q_{i,n}[s]$. We denote the energy per symbol for D2D pair i on subcarrier n by $\mathcal{E}_{i,n}$, and let the Kronecker delta function be δ_x. The in-phase and quadrature components of the l-th complex data symbol on the n-th subcarrier of the i-th transmitter are denoted by $X^I_{i,n}[l]$ and $X^Q_{i,n}[l]$, respectively, where

$$\begin{aligned} E[X^I_{i_1,n_1}[l_1]X^I_{i_2,n_2}[l_2])] &= E[X^Q_{i_1,n_1}[l_1]X^Q_{i_2,n_2}[l_2]] \\ &= \mathcal{E}_{i_1,n_1}\delta_{i_1-i_2}\delta_{n_1-n_2}\delta_{l_1-l_2}, \end{aligned} \tag{2}$$

and the in-phase and quadrature components are uncorrelated.

The system adopts a filtered multitone (FMT) waveform. Let $G(t)$ be the Fourier transform of $g(t)$, then $|G(f)|^2$ is a Nyquist pulse with roll-off factor $0 < \beta \leq 1$. The frequency spacing of adjacent subcarriers is $F_0 = (1+\beta)/T_0$, so the spectra of adjacent subcarriers do not overlap and intercarrier interference does not exist.

We use a block fading channel model, in which the coherence bandwidth f_{coh} is larger than the bandwidth of a subcarrier, and the coherence time T_{coh} is larger than the duration of a symbol but much smaller than the duration T_{GOP} of a group of pictures (GOP). The complex channel response on subcarrier m from the i-th transmitter to the k-th receiver is denoted by $h_{i,k,m} = \sqrt{H_{i,k}}\tilde{h}_{i,k,m}$, where $H_{i,k}$ denotes the average channel gain due to large scale fading, and $\tilde{h}_{i,k,m}$ is the channel response due to multipath fading. The large scale fading includes path loss and shadowing, and

is constant over a GOP. The multipath fading is modeled as Rayleigh fading, so $\tilde{h}_{i,k,m}$ is circularly symmetric complex Gaussian (CSCG) with zero mean and unit variance. We further assume that multipath fading is independent for different D2D pairs.

The signal from the i-th transmitter arrives at the k-th receiver with a time delay $\tau_{i,k}$ compared to the desired signal from the k-th transmitter ($i, k = 1, 2, \cdots, K$), where $\tau_{i,k}$ modulo T_0 is uniformly distributed in $[0, T_0)$, if $i \neq k$. Also, $|\tau_{i,k}| \ll T_{\text{GOP}}$. We assume that a coherent receiver is implemented and the receiver maintains perfect bit synchronization and phase recovery for the desired signal, so we set $\tau_{k,k} = 0$. Therefore, the lowpass equivalent signal at the k-th receiver is given by

$$y_k(t) = \sum_{i=1}^{K} \sum_{n=1}^{M_c} \sum_{s} h_{i,k,n} X_{i,n}[s]\, g(t - \tau_{i,k} - sT_0) \cdot e^{j2\pi n F_0 (t-\tau_{i,k})} + n_k(t), \quad (3)$$

where $n_k(t)$ is complex AWGN at the k-th receiver with two-sided power spectral density N_0. A matched filter is used at subcarrier m of the k-th receiver. The output of the matched filter for the l-th received symbol is given by

$$Y_{k,m}[l] = \int_{-\infty}^{\infty} y_k(t) e^{-j2\pi m F_0 t} g^*(t - lT_0) dt. \quad (4)$$

B. Adaptive Modulation

Substituting (1), (3) into (4), the output for the l-th received symbol is given by

$$Y_{k,m}[l] = \sum_{i=1}^{K} \sum_{s} h_{i,k,m} X_{i,m}[s] e^{-j2\pi \tau_{i,k}} \cdot \int_{-\infty}^{\infty} g(t - \tau_{i,k} - sT_0) g^*(t - lT_0) dt + N_{k,m}[l], \quad (5)$$

where the noise term is given by $N_{k,m}[l] = \int_{-\infty}^{\infty} n_k(t) e^{-j2\pi m F_0 t} g^*(t - lT_0) dt$, which is a zero-mean CSCG random variable with variance $N_0 \int_{-\infty}^{\infty} |g(t)|^2\, dt = N_0$. Substituting $\tau_{k,k} = 0$ and $\int_{-\infty}^{\infty} |g(t)|^2 dt = 1$ into (5), we have

$$Y_{k,m}[l] = h_{k,k,m} X_{k,m}[s] + \sum_{i=1, i\neq k}^{K} h_{i,k,m} \sum_{s} X_{i,m}[s] e^{-j2\pi \tau_{i,k}} \cdot \int_{-\infty}^{\infty} g(t - \tau_{i,k} - sT_0) g^*(t - lT_0) dt + N_{k,m}[l]. \quad (6)$$

where the second term is the co-channel interference. From [13], we have

$$E\left[\left| \sum_{s} X_{i,m}[s] e^{-j2\pi \tau_{i,k}} \int_{-\infty}^{\infty} g(t - \tau_{i,k} - sT_0) g^* (t - lT_0) dt \right|^2 \right] = \mathcal{E}_{i,m} \left(1 - \frac{\beta}{4}\right). \quad (7)$$

From (6) and (7), the power of co-channel interference is given by

$$P_I = \sum_{i=1, i\neq k}^{K} E[|h_{i,k,m}|^2] \mathcal{E}_{i,m} \left(1 - \frac{\beta}{4}\right) = \left(1 - \frac{\beta}{4}\right) \sum_{i=1, i\neq k}^{K} H_{i,k} \mathcal{E}_{i,m}. \quad (8)$$

We consider a fixed power, variable rate scheme, in which the transmission powers of all D2D transmitters are constant over a GOP, and D2D receivers adaptively select the alphabet sizes according to the instantaneous SINR. The transmission power varies for different D2D pairs. Given the channel response of the desired channel $h_{k,k,m}$, the instantaneous SINR on the m-th subcarrier of the k-th receiver is given by

$$\gamma_{k,m}(h_{k,k,m}) = \frac{|h_{k,k,m}|^2 \mathcal{E}_{k,m}}{\left(1 - \frac{\beta}{4}\right) \sum_{i=1, i\neq k}^{K} H_{i,k} \mathcal{E}_{i,m} + N_0}. \quad (9)$$

Eq. (9) is the expression for the instantaneous SINR, which is a function of the channel gain of the desired signal. Interferences arrive at the D2D receiver with random delays, and the delays are modeled as independent random variables for different interferers. Based on the block fading model that we use, the instantaneous interference channel gain can vary within the coherence time of the desired signal, and thereby is random, even if conditioned on the channel gain of the desired signal. As the number of interferers is large and no interferer dominates, the composite effect of multiple interferers of random power is modeled as an additional Gaussian noise source. Given $h_{k,k,m}$, the symbol error rate (SER) of square QAM with alphabet size $M_{k,m}$ for the instantaneous SINR $\gamma_{k,m}$ is approximated by [9]

$$\begin{aligned} &\text{SER} \\ &\approx 4Q\left(\sqrt{\frac{3\,\gamma_{k,m}(h_{k,k,m})}{M_{k,m} - 1}}\right) \\ &= 4Q\left(\sqrt{\frac{3}{M_{k,m} - 1} \cdot \frac{|h_{k,k,m}|^2 \mathcal{E}_{k,m}}{\left(1 - \frac{\beta}{4}\right) \sum_{i=1, i\neq k}^{K} H_{i,k} \mathcal{E}_{i,m} + N_0}}\right). \end{aligned} \quad (10)$$

Therefore, given $h_{k,k,m}$, the number of bits per symbol for a SER target is obtained as

$$\begin{aligned} &\tilde{R}_{k,m} \\ &= \min\left\{ \left\lfloor \log_2\left(1 + \frac{\eta |h_{k,k,m}|^2 \mathcal{E}_{k,m}}{\left(1 - \frac{\beta}{4}\right) \sum_{i=1, i\neq k}^{K} H_{i,k} \mathcal{E}_{i,m} + N_0}\right) \right\rfloor, \right. \\ &\qquad \left. \log_2(M_{\max}) \right\}, \end{aligned} \quad (11)$$

where $\eta \triangleq 3 / \left[Q^{-1}\left(\text{SER}_{\text{target}}/4\right)\right]^2$ is a positive constant determined by the SER target, and $M_{\max}$ is the largest alphabet size allowed by the system.

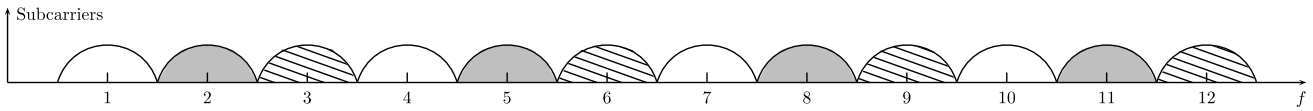

Fig. 2. Groups of subcarriers for $M_c = 12$, $N = 3$, $M_g = 4$.

Since $h_{k,k,m} = \sqrt{H_{k,k}}\tilde{h}_{k,k,m}$ and $\tilde{h}_{k,k,m}$ is a CSCG random variable with unity variance, $\gamma \triangleq |\tilde{h}_{k,k,m}|^2$ satisfies an exponential distribution with unity variance. If we ignore the flooring operation, the average number of bits per symbol is given by

$$R_{k,m} \triangleq E[\tilde{R}_{k,m}] \approx \min\left\{\int_0^\infty \log_2\left(1+\eta\overline{\gamma}_{k,m}\gamma\right)e^{-\gamma}d\gamma,\ \log_2(M_{\max})\right\}, \tag{12}$$

where $\overline{\gamma}_{k,m}$ is the average SINR of D2D pair k on subcarrier m, given by

$$\overline{\gamma}_{k,m} \triangleq \frac{H_{k,k}\mathcal{E}_{k,m}}{\left(1-\frac{\beta}{4}\right)\sum_{i=1,i\neq k}^{K} H_{i,k}\mathcal{E}_{i,m}+N_0}. \tag{13}$$

From [15, eq. (34)], we obtain

$$f(x) \triangleq \int_0^\infty \log_2\left(1+\frac{\gamma}{x}\right)e^{-\gamma}d\gamma = \log_2(e)\,e^x E_1(x), \tag{14}$$

where $f(\cdot)$ maps a power ratio (the reciprocal of average SINR) to the average number of bits per symbol. $E_1(x)$ is the exponential integral of the first order, defined by $E_1(x) = \int_x^\infty e^{-t}/t\,dt,\ x > 0$. The average number of bits per symbol is finally given by

$$R_{k,m}(\overline{\gamma}_{k,m}) \approx \min\left\{f\left(\frac{1}{\eta\overline{\gamma}_{k,m}}\right),\ \log_2(M_{\max})\right\}. \tag{15}$$

Since the integrand in (14), $\log_2(1+\gamma/x)e^{-\gamma}$, is positive and monotonically decreasing in x for $\gamma > 0$, $f(x)$ is positive and monotonically decreasing in x. Therefore, $f(1/(\eta\overline{\gamma}_k))$ is positive and monotonically increasing in $\overline{\gamma}_k$.

C. Scalable Video Codec

The D2D videos are encoded with the scalable video coding extension of H.264/AVC with medium granular scalability (MGS) [16]. The video bitstream is organized in the unit of GOP. In each bitstream, the most important video information is conveyed by the base layer, and other video information of diminishing importance is contained in the successive enhancement layers. With a scalable video codec, the decoder needs only a portion of the encoded bitstream to display the video. Decoded fidelity of the video depends on the length of the bitstream and the rate distortion characteristics of the video content. The mean square error (MSE) of the video diminishes as more enhancement layers are received. Video packets are transmitted in the order of descending priority. If an error occurs during transmission, that packet and all successive packets in the GOP will be dropped, but previous packets will be used for decoding the GOP.

The rate-distortion (RD) function of the video characterizes the tradeoff between the video distortion and the number of bits used to compress the raw video data. Since the video is compressed on a GOP-by-GOP basis, this RD function is also measured for each GOP. The MSE distortion D_k can be approximated as a function of the number of correctly received video bits B_k in the GOP, written as [17]

$$\text{MSE}_k = a_k + \frac{b'_k}{B_k + c'_k}, \tag{16}$$

where a_k, b'_k, and c'_k are positive constants determined by curve fitting and are dependent on the video content. We assume that one GOP is transmitted in each time slot, thus T_{GOP} equals the duration of the time slot. The video bits are protected by a FEC code with fixed rate u. The average number of coded bits per symbol transmitted on the m-th subcarrier of the k-th link is $R_{k,m}$, and $R_{k,m}$ can be zero for some k and m. The number of video bits (B_k) transmitted on the k-th link in a time slot is given by

$$B_k = \frac{uT_{\text{GOP}}}{T_0}\sum_{m=1}^{M_c} R_{k,m}. \tag{17}$$

For simplicity of notation, we define $\tilde{b}_k \triangleq b'_k T_0/(uT_{\text{GOP}})$, $\tilde{c}_k \triangleq c'_k T_0/(uT_{\text{GOP}})$. Substituting (17) into (16), the MSE of the GOP at the video decoder can be further written as

$$\text{MSE}_k = a_k + \frac{\tilde{b}_k}{\sum_{m=1}^{M_c} R_{k,m} + \tilde{c}_k}. \tag{18}$$

III. Subcarrier Assignment and Power Allocation

A. Subcarrier Assignment

We divided subcarriers into groups to simplify the subcarrier assignment procedure. The frequency band of the system, W (Hz), is equally divided into $M_c = NM_g$ subcarriers, where there are N groups of subcarriers ($N < K$) and a group consists of M_g interleaved subcarriers, as shown in Fig. 2. More specifically, group n consists of subcarriers n, $n+N, \cdots, n+(M_g-1)N$, where $n = 1, 2, \cdots, N$. Each D2D pair can be assigned to at most one group of subcarriers. The groups of subcarriers are determined in advance and are not optimization parameters.

The system operates in a time-slotted manner, with a single GOP transmitted in each time slot. The duration of a GOP, T_{GOP}, is a constant. The subcarrier assignment and power allocation decision is made by the BS at the beginning of each GOP, and is fixed for the entire GOP. The BS is able to collect the average channel gain ($H_{i,k}$) of the desired and interference signals and video RD information from the D2D pairs via the control channel.

Each D2D pair is assigned to at most one group of subcarriers for complexity concerns. This one-group constraint guarantees convexity of the power allocation problem, such that the BS can conduct an efficient search ending up with a high-quality power allocation solution. If a D2D pair can be assigned to more than one group of subcarriers, the convex structure does not exist, and it either requires an exhaustive search for the optimal power allocation which is extremely complex, or it typically ends up at an inferior local optimum. An example of the latter is given by the heuristic power allocation algorithm later in Section IV-C. Its performance is considerably worse than the algorithms using the one-group constraint.

Each transmitter allocates equal power into each assigned subcarrier. The indices of D2D pairs are randomized at the beginning of each GOP. While groups 1 to N stand for sets of subcarriers, we also use group 0 for simplicity of notation: a D2D pair assigned to group 0 does not transmit. The proposed subcarrier assignment algorithm is as follows:

- Step 1: Initialization.
  - Step 1.1: Assign D2D pairs $1, 2, \cdots, N$ to groups $1, 2, \cdots, N$, respectively.
  - Step 1.2: Sequentially consider D2D pairs $N+1$, $N+2, \cdots, K$. For each D2D pair i, iterate over groups $n = 0, 1, 2, \cdots, N$, and consider assigning D2D pair i to group n. Notice that the subcarrier assignments of D2D pairs $1, 2, \cdots, i-1$ have already been made, so we run the cross-layer power allocation algorithm based on the subcarrier assignments of D2D pairs $1, 2, \cdots, i-1$. Assign D2D pair i to the group that minimizes the total video MSE.
- Step 2: Subcarrier reassignment. Sequentially consider D2D pairs $1, 2, \cdots, K$: For each group $n = 0, 1, 2, \cdots, N$ to which D2D pair i is not assigned, consider reassigning D2D pair i into group n instead, and run the cross-layer power allocation algorithm. Reassign D2D pair i into group n if the total video MSE decreases.

The subcarrier assignment algorithm calls the power allocation algorithm $[(K-N)(N+1)+K(N+1)]$ times. Every time the power allocation algorithm is called in the search for group n, the temporary subcarrier assignment in group n and the index of the D2D pair newly added to group n are passed to the cross-layer power allocation algorithm as the input. The indices of D2D pairs in group n are denoted by $\mathcal{J}_n = \{j_1^{(n)}, j_2^{(n)}, \cdots, j_{K_n}^{(n)}\}$, where K_n is the number of D2D pairs in group n and $n = 0, 1, 2, \cdots, N_g$. We also denote $\mathcal{K}_n \triangleq \{1, 2 \cdots, K_n\}$.

B. Analysis for Cross-Layer Power Allocation

The cross-layer power allocation is formulated as a total video MSE minimization problem, given the subcarrier assignment. The optimization parameter is the transmission power of each D2D pair. The average channel gains, the video RD and the largest transmission power of a D2D pair are known constants in the optimization. The cross-layer power allocation problem for D2D pairs assigned to a given group n $(1 \le n \le N)$ is formally written as

$$\begin{aligned} &\text{minimize} \sum_{j\in\mathcal{J}_n}\left(a_j + \frac{\tilde{b}_j}{\sum_{m\in\{n,\ n+N,\cdots,n+(M_g-1)N\}} r_{j,m} + \tilde{c}_j}\right) \\ &\text{subject to } 0 \le r_{j,m} \le R_{j,m}(\overline{\gamma}_{j,m}),\ 0 \le M_g\mathcal{E}_j/T_0 \le P, \\ &\qquad \forall j \in \mathcal{J}_n,\ \forall m \in \{n,\ n+N, \cdots,\ n+(M_g-1)N\} \\ &\text{variables } r_{j,m},\ \mathcal{E}_j \end{aligned} \tag{19}$$

where $R_{j,m}(\overline{\gamma}_{j,m})$ is the average number of bits per symbol on subcarrier m of D2D pair j, and is given by (15) as a function of the average SINR $(\overline{\gamma}_{j,m})$. $\mathcal{E}_j$ is the symbol energy of D2D pair j on each assigned subcarrier, so $M_g\mathcal{E}_j/T_0$ is the total transmission power of D2D transmitter j, and the total transmission power of a D2D transmitter is upper bounded by the total transmission power constraint P.

For each D2D pair in group n, since equal power is allocated to assigned subcarriers $m \in \{n,\ n+N, \cdots,\ n+(M_g-1)N\}$, the average SINR $\overline{\gamma}_{j,m}$ from (13) is equal for each assigned subcarrier. Therefore, we can omit the subscript m in the notation of $\overline{\gamma}_{j,m}$ and the average SINR of D2D pair j on each subcarrier can be written as

$$\overline{\gamma}_j = \frac{H_{j,j}\mathcal{E}_j}{\left(1-\frac{\beta}{4}\right)\sum_{i\in\mathcal{J}_n/j} H_{i,j}\mathcal{E}_i + N_0}, \quad j \in \mathcal{J}_n. \tag{20}$$

Similarly, we can omit the subscript m in the notation of $r_{j,m}$ and it can be written as r_j. Substituting (15) into (19), we rewrite (19) as

$$\begin{aligned} &\text{minimize} \sum_{j\in\mathcal{J}_n} \frac{\tilde{b}_j}{M_g r_j + \tilde{c}_j} \\ &\text{subject to } 0 \le r_j \le \min\left\{ f\left(\frac{1}{\eta\overline{\gamma}_j}\right), \log_2(M_{\max})\right\}, \\ &\qquad 0 \le M_g\mathcal{E}_j/T_0 \le P, \quad \forall j \in \mathcal{J}_n \end{aligned} \tag{21}$$

where $f(\cdot)$ is a mapping from a power ratio (the reciprocal of average SINR) to the average number of bits per symbol given by (14), and $f(\cdot)$ monotonically decreases, so the inverse function of $f(\cdot)$, denoted by $f^{-1}(\cdot)$, exists. Specifically, $f(e^{-x})$ monotonically increases in x, and the inverse function of $y = f(e^{-x})$ is $x = -\ln[f^{-1}(y)]$.

Consider variable transformations $b_k \triangleq \tilde{b}_{j_k^{(n)}}/M_g$, $c_k \triangleq \tilde{c}_{j_k^{(n)}}/M_g$, $z_k \triangleq \ln(\mathcal{E}_{j_k^{(n)}})$ and $s_k \triangleq -\ln[f^{-1}(r_{j_k^{(n)}})]$, where $k \in \mathcal{K}_n$. Since $r_{j_k^{(n)}} \ge 0$ is the average number of bits per symbol, $1/f^{-1}(r_{j_k^{(n)}}) \ge 0$ is the average SINR and hence $s_k \in (-\infty, +\infty)$ is proportional to the average SINR in dB. With this variable transformation, we can rewrite (21) as

$$\begin{aligned} &\text{minimize} \sum_{k=1}^{K_n} \frac{b_k}{f\left(e^{-s_k}\right) + c_k} \\ &\text{subject to (C1) } s_k \le s_{\text{sat}} \triangleq -\ln[f^{-1}(\log_2(M_{\max}))],\ \forall k \in \mathcal{K}_n \\ &\qquad \text{(C2) } s_k \le \ln(\eta\overline{\gamma}_{j_k^{(n)}}),\ z_k \le \ln(PT_0/M_g),\ \forall k \in \mathcal{K}_n \end{aligned} \tag{22}$$

which is a constrained minimization problem with variables $\{s_1, s_2, \cdots, s_{K_n}, z_1, z_2, \cdots, z_{K_n}\}$.

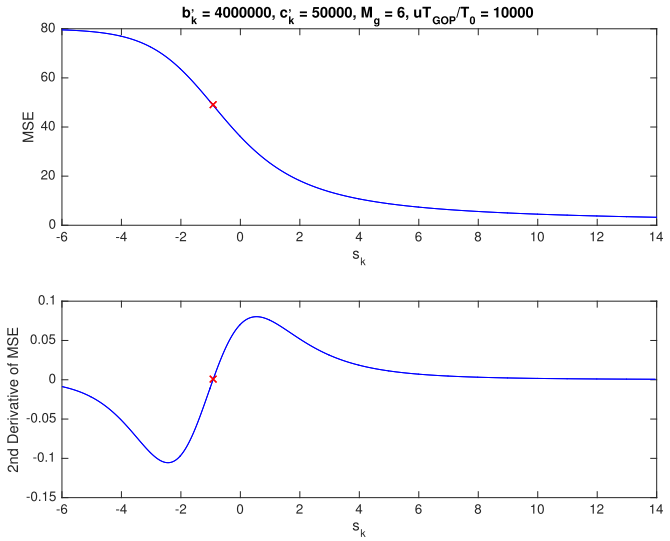

Fig. 3. An example of the video MSE as a function of s_k. The inflection point s_k^* is marked as a "x".

1) Property of Feasible Region: The feasible region $\mathcal{S}$ is defined as the set of all vectors $\underline{s} = (s_1, \cdots, s_{K_n})$ that satisfy constraints (C1) and (C2) in (22).

To prove (C2) forms a convex region in $(s_1, \cdots, s_{K_n})$, we substitute $\mathcal{E}_{j_k^{(n)}} = \exp(z_k)$ into (20), which yields

$$\overline{\gamma}_{j_k^{(n)}} = \frac{H_{j_k^{(n)}, j_k^{(n)}} e^{z_k}}{\left(1 - \frac{\beta}{4}\right) \sum_{i=1,\ i\neq k}^{K_n} H_{j_i^{(n)}, j_k^{(n)}} e^{z_i} + N_0}, \quad k \in \mathcal{K}_u. \tag{23}$$

We substitute (23) into constraint (C2) in (22), and obtain

$$\begin{aligned} s_k &\le \ln\left[\frac{\eta H_{j_k^{(n)}, j_k^{(n)}} e^{z_k}}{\left(1 - \frac{\beta}{4}\right) \sum_{i=1,\ i\neq k}^{K_n} H_{j_i^{(n)}, j_k^{(n)}} e^{z_i} + N_0}\right], \\ z_k &\le \ln(PT_0/M_g), \quad \forall k \in \mathcal{K}_u, \end{aligned} \tag{24}$$

which reduces to

$$\begin{aligned} &\ln\left\{\left(1 - \frac{\beta}{4}\right) \sum_{i=1,\ i\neq k}^{K_n} H_{j_i^{(n)}, j_k^{(n)}} e^{z_i - z_k} + N_0 e^{-z_k}\right\} + s_k \\ &\quad \le \ln(\eta H_{j_k^{(n)}, j_k^{(n)}}), \quad z_k \le \ln(PT_0/M_g), \ \forall k \in \mathcal{K}_u. \end{aligned} \tag{25}$$

Denote $\underline{z} \triangleq (z_1, z_2, \cdots, z_{K_n})$ and $\underline{x}^{(k)} \triangleq (x_1^{(k)}, x_2^{(k)}, \cdots, x_{K_n}^{(k)})$. We observe that the first term in (25) is the composition of a log-sum-exp function $\ln[\sum_{i=1}^{K_n} e^{x_i^{(k)}}]$ and an affine mapping:

$$x_i^{(k)} = \begin{cases} z_i - z_k + \ln\left[\left(1 - \frac{\beta}{4}\right) H_{j_i^{(n)}, j_k^{(n)}}\right], \\ \qquad\qquad \text{if } i \neq k, \ k \in \mathcal{K}_u, \\ -z_k + \ln(N_0), \quad \text{if } i = k, \ k \in \mathcal{K}_u. \end{cases} \tag{26}$$

The log-sum-exp function $\ln[\sum_{i=1}^{K_n} e^{x_i^{(k)}}]$ is convex in $\underline{x}^{(k)}$ [18]. Therefore, the first term in (25) is a composition of a convex function with an affine mapping, and thereby is a convex function in $\underline{z}$ [18]. Consequently, (25) is convex in $(\underline{s}, \underline{z})$ and thereby is convex in $\underline{s}$, which indicates that constraint (C2) is convex.

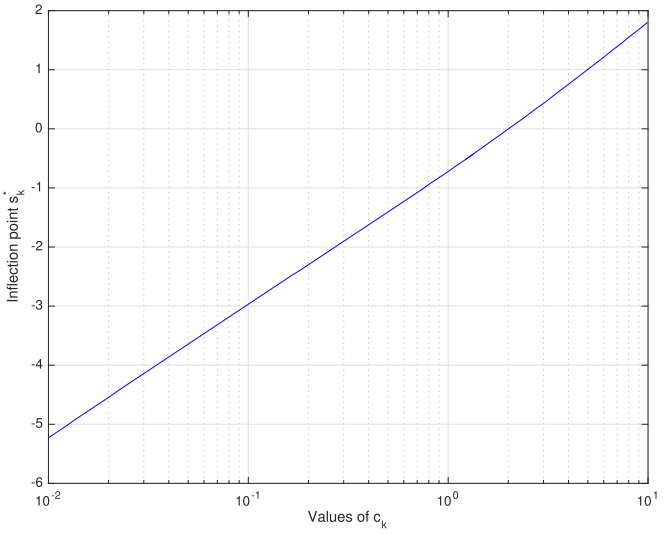

Fig. 4. Inflection point s_k^* as a function of c_k.

In addition, the halfspaces specified by constraint (C1) are convex regions in $(s_1, \cdots, s_{K_n})$ [18]. Now that we have proved both constraints (C1) and (C2) in (22) are convex regions, the feasible region $\mathcal{S}$ is a convex region in $(s_1, \cdots, s_{K_n})$.

To give a general idea of the shape of region $\mathcal{S}$, we can easily identify a rectangular region that contains $\mathcal{S}$. From (20), the average SINR of D2D pair $j_k^{(n)}$ is upper bounded by

$$\overline{\gamma}_{j_k^{(n)}} \le \frac{H_{j_k^{(n)}, j_k^{(n)}} PT_0}{M_g N_0} \triangleq \gamma_{k,\max}. \tag{27}$$

Therefore, letting $s_{k,\max} \triangleq \min\{\ln(\eta\gamma_{k,\max}), s_{\text{sat}}\}$, we have $\mathcal{S} \subset \{(s_1, \cdots, s_{K_n}) | s_k \le s_{k,\max}, \forall k \in \mathcal{K}_u\}$.

The equality in (27) is achieved when D2D pair k is transmitted with the largest power and all other users sharing the subcarriers with D2D pair k use no transmission power. Let $\underline{s}_k^{\max} = (\underbrace{-\infty, \cdots, -\infty}_{k-1}, s_{k,\max}, \underbrace{-\infty, \cdots, -\infty}_{K_n - k})$, which indicates that D2D pair $j_k^{(n)}$ transmits at the largest power and other D2D pairs do not transmit, thereby $\underline{s}_k^{\max} \in \mathcal{S}$.

The boundary of $\mathcal{S}$ does not have an explicit expression, however, we can check if a vector $\underline{s} = (s_1, s_2, \cdots, s_{K_n})$ satisfies $\underline{s} \in \mathcal{S}$. We let $s_k = \ln(\eta\overline{\gamma}_{j_k^{(n)}})$ according to (C2) in (22), then $\overline{\gamma}_{j_k^{(n)}} = e^{s_k}/\eta$. From (20), we obtain

$$\frac{H_{j_k^{(n)}, j_k^{(n)}} \mathcal{E}_{j_k^{(n)}}}{\left(1 - \frac{\beta}{4}\right) \sum_{i=1,\ i\neq k}^{K_n} H_{j_i^{(n)}, j_k^{(n)}} \mathcal{E}_{j_i^{(n)}} + N_0} = \overline{\gamma}_{j_k^{(n)}} = \frac{e^{s_k}}{\eta}, \tag{28}$$

which yields a set of equations of symbol energy $\{\mathcal{E}_{j_k^{(n)}}\}$:

$$\left(1 - \frac{\beta}{4}\right) \sum_{i=1,\ i\neq k}^{K_n} H_{j_i^{(n)}, j_k^{(n)}} \mathcal{E}_{j_i^{(n)}} + N_0 = \eta e^{-s_k} H_{j_k^{(n)}, j_k^{(n)}} \mathcal{E}_{j_k^{(n)}}. \tag{29}$$

If $\underline{s} \in \mathcal{S}$, the corresponding symbol energy $\{\mathcal{E}_{j_k^{(n)}}\}$ should satisfy the power constraint. Therefore, the following steps can determine whether $\underline{s} \in \mathcal{S}$:

- First step is to check simple bounds: if $\exists k \in \mathcal{K}_u$ such that $s_k > s_{k,\max}$, then $\underline{s} \notin \mathcal{S}$; otherwise, proceed to next step.

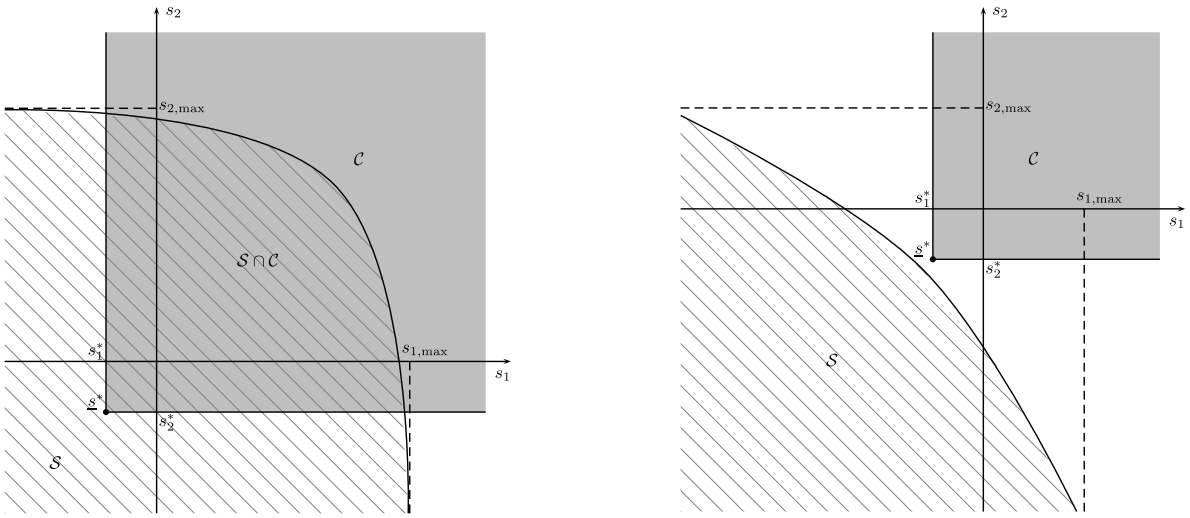

Fig. 5. Region $\mathcal{C}$ and feasible region $\mathcal{S}$ for a two-user case. The left and right figures show the cases of $\mathcal{S}\cap\mathcal{C}\neq\varnothing$ and $\mathcal{S}\cap\mathcal{C}=\varnothing$, respectively. The boundary of $\mathcal{C}$ is given by $s_k > s_k^*$, $\forall k\in\mathcal{K}_a$, where s_k^* is determined by c_k using a look-up table.

- The second step is substituting $\{s_k\}$ into (29) and solving for $\{\mathcal{E}_{j_k^{(n)}}\}$. If $0\le\mathcal{E}_{j_k^{(n)}}\le PT_0/M_g$, $\forall k\in\mathcal{K}_a$, then the vector $\underline{s}\in\mathcal{S}$; if there exists $k\in\mathcal{K}_a$ such that $\mathcal{E}_{j_k^{(n)}}<0$ or $\mathcal{E}_{j_k^{(n)}}>PT_0/M_g$, then the vector $\underline{s}\notin\mathcal{S}$.

2) Property of Objective Function: The following proposition characterizes a key property of the objective function in (22): The objective function is convex if the SINR of each D2D user exceeds a threshold. The threshold is determined by c_k. Here c_k is a parameter dependent on both video rate-distortion and the number of subcarriers in a group.

Proposition 1: Let y_k^* be the smallest root of

$$e^y E_1(y)=\frac{1}{2y(y-1)}\Big\{[(y+1)c_k\ln(2)+3]y -\sqrt{y[(\ln(2)c_k)^2y(y+1)^2+y+2\ln(2)c_k y(y+5)+8]}\Big\} \tag{30}$$

in $y>0$, and denote the video MSE of D2D pair $j_k^{(n)}$ by

$$g_k(s_k)\triangleq\frac{b_k}{f\left(e^{-s_k}\right)+c_k}. \tag{31}$$

Then:

1) y_k^* always exists and is only dependent on c_k;
2) The second derivative of $g_k(s_k)$, denoted by $g_k''(s_k)$, has a real root $s_k^*\triangleq-\ln(y_k^*)$ and $g_k''(s_k)>0$ for $s_k>s_k^*$.

Proof: The proof is given in the appendix. ■

As a result of Proposition 1, the video MSE of D2D pair $j_k^{(n)}$, $g_k(s_k)$ is convex in $s_k>s_k^*$, where s_k^* is the inflection point, as presented in Fig. 3. s_k^* is a function of c_k, and their relation is shown in Fig. 4. In our algorithm, we find s_k^* for a given value of c_k offline by a bisection search, and create a one-dimensional look-up table for s_k^* as a function of c_k.

Let $\mathcal{C}$ be the set of all vectors $\underline{s}=(s_1,s_2,\cdots,s_{K_n})$ over which the objective function of (22) is convex. From Proposition 1, $\mathcal{C}=\{(s_1,\cdots,s_{K_n})|s_k>s_k^*,\ \forall k\in\mathcal{K}_a\}$, which is the intersection of half-spaces, thereby being a convex set. Since s_k^* always exists $\forall k\in\mathcal{K}_a$, region $\mathcal{C}$ also always exists. The objective function is convex in region $\mathcal{C}$, and is non-convex outside region $\mathcal{C}$.

C. Proposed Cross-Layer Power Allocation Algorithm

The proposed power allocation algorithm aims to minimize the total video MSE based on the video RD and average channel gain. There are two scenarios as shown in Fig. 5. The proposed algorithm searches for a local optimum in $\mathcal{S}\cap\mathcal{C}$, if $\mathcal{S}\cap\mathcal{C}\neq\varnothing$. If $\mathcal{S}\cap\mathcal{C}=\varnothing$, the algorithm keeps the transmission power of the existing D2D pairs in the current group unchanged and searches for a locally optimal transmission power for the newly added D2D pair. Notice that $\mathcal{S}\cap\mathcal{C}=\varnothing$ is equivalent to $\underline{s}^*\triangleq(s_1^*,s_2^*,\cdots,s_{K_n}^*)\notin\mathcal{S}$. Therefore, to determine whether $\mathcal{S}\cap\mathcal{C}=\varnothing$, we only need to check if $\underline{s}^*\in\mathcal{S}$.

If $\underline{s}^*\in\mathcal{S}$, we aim to find the local optimum in $\mathcal{S}\cap\mathcal{C}$. Since $\mathcal{S}\cap\mathcal{C}$ is convex and the objective function of (22) is also convex in $\mathcal{S}\cap\mathcal{C}$, many well-established algorithms can be implemented to find the optimal solution to (22) in $\mathcal{S}\cap\mathcal{C}$. For example, the interior point method [18] can be used, whose complexity is $O(\sqrt{K_n})$.

If $\underline{s}^*\notin\mathcal{S}$, while keeping the transmission power of all existing D2D pairs in the current group unchanged, we search for a local optimum for the transmission power of the newly added user using coordinated descent [19].

Here we summarize the proposed cross-layer power allocation algorithm:

- Step 1: For each $k\in\mathcal{K}_a$, we find values of s_k^* from the entries in the look-up table (Fig. 4) corresponding to c_k.
- Step 2: Check if $\underline{s}^*$ is feasible. If so, go to Step 3a; otherwise, go to Step 3b.
- Step 3a: We first let $s_k:=s_{k,\max}$, $\forall k\in\mathcal{K}_a$. We repeatedly update $s_k:=(s_k+s_k^*)/2$ until $(s_1,\cdots,s_{K_n})$ is feasible.

With $(s_1, \cdots, s_{K_n})$ as the initialization, the interior point method can be applied to (22) with (C2) replaced by (25). It will converge to a local optimum in region $\mathcal{S} \cap \mathcal{C}$ for the cross-layer power allocation problem (22), and the cross-layer power allocation algorithm terminates.

- Step 3b: We keep the transmission power of all existing D2D pairs in the current group unchanged. We initialize the transmission power of the newly added D2D pair to zero, and repeatedly update the transmission power of the newly added D2D pair using gradient descent [19], subject to the power constraint, until the decrease of total MSE is less than a threshold, and then terminate the cross-layer power allocation algorithm.

The complexity of the proposed power allocation inner-loop is mainly from the interior point method, whose complexity is $O(\sqrt{K_n})$. Recall that the proposed subcarrier assignment outer-loop calls the power allocation inner-loop $[(K-N)(N+1)+K(N+1)]$ times, so the overall complexity of the proposed algorithm is upper bounded by $O(K^{\frac{3}{2}}N)$. As a comparison, the subcarrier assignment outer-loop and power allocation inner-loop in [5] both have a complexity of $O(KN)$, so the overall complexity is $O(K^2N^2)$.

IV. Baseline Algorithms

A. Other Methods for Local Search in Subcarrier Assignment

Step 2 of the proposed subcarrier assignment algorithm uses one round of subcarrier reassignment for local search. We consider comparing this approach with other local search methods in terms of complexity and performance.

We first consider replacing one round of subcarrier reassignment by one round of subcarrier swapping. Specifically, in Step 2 of the subcarrier assignment algorithm, we use the following operations instead:

- [One round of swapping] For each D2D pair $i = 1, 2, \cdots, K$, we consider each D2D pair j that is not assigned to D2D pair i's group, and assess the total MSE of swapping the subcarrier assignment of D2D pairs i and j by calling the cross-layer power allocation algorithm, and then swapping the group assignment if the total video MSE decreases.

We also consider replacing Step 2 of the original subcarrier assignment algorithm by repeatedly reassigning a D2D pair into a different group, until the total MSE does not decrease. The detailed local search step is given as follows:

- [Multiple rounds of reassignment] We first create a list of all D2D pairs. We repeat the following steps until all D2D pairs are removed from the list: For each D2D pair $i = 1, 2, \cdots, K$ on the list, we let n iterate over the indices of all groups that D2D pair i is not assigned to, and assess the total MSE of reassigning D2D pair i into group n by calling the cross-layer power allocation algorithm. If the total MSE decreases, we reassign D2D pair i into group n, put all D2D pairs in group n on the list, and remove the duplicated indices on the list. If the total MSE does not decrease after iterating over all n, we remove D2D pair i from the list.

Similarly, we consider replacing Step 2 of the original subcarrier assignment algorithm by repeatedly swapping the assignment of two D2D pairs, until the total MSE does not decrease:

- [Multiple rounds of swapping] We first create a list of all D2D pairs. We repeat the following steps until all D2D pairs are removed from the list: For each D2D pair $i = 1, 2, \cdots, K$ on the list, we let j iterate over the indices of all D2D pairs that are not in D2D pair i's group, and assess the total MSE of swapping the subcarrier assignment of D2D pairs i and j by calling the cross-layer power allocation algorithm. If the total MSE decreases, we swap the subcarrier assignment of D2D pairs i and j, put all D2D pairs in these two groups on the list, and remove the duplicated indices on the list. If the total MSE does not decrease after iterating over all j, we remove D2D pair i from the list.

B. Cross-Layer Subcarrier Assignment With Maximal Transmission Power

To demonstrate the performance improvement of our proposed cross-layer power allocation, we consider a baseline algorithm in which all D2D pairs transmit with the maximal transmission power, with power equally allocated on all assigned subcarriers. The subcarrier assignment outer loop remains the same as the proposed algorithm.

C. Heuristic Subcarrier Assignment Without Grouping

In Section III B, given that a set of subcarriers is assigned to a set of D2D pairs exclusively and equal power is allocated to subcarriers of each D2D pair, the cross-layer power allocation problem is shown to have a tractable convex structure. In contrast, if D2D pairs are allowed to use arbitrary sets of subcarriers, such as overlapping but non-identical sets of subcarriers, the cross-layer power allocation problem is non-convex [13], and the algorithm to search for the global minimum, such as exhaustive search, has a complexity that is exponential in K and M_c, and thereby the resultant complexity of searching for the global minimum is prohibitive, even for offline computation. Therefore, a heuristic algorithm with a polynomial complexity in K and M_c is of interest. The following heuristic algorithm is considered as a baseline, in which equal transmission power is allocated to all assigned subcarriers of each D2D pair and the total transmission power of each D2D pair is set to P for simplicity:

- Step 1: Each subcarrier is initially assigned to the D2D pair with the best instantaneous channel response.
- Step 2: We choose the D2D pair with the steepest RD slope.
- Step 3: We iterate over all subcarriers that are not assigned to the chosen D2D pair. If the total MSE decreases when the chosen user acquires the current subcarrier, we assign this subcarrier to the chosen user.
- Step 4: We let i iterate over the subcarriers that are assigned to the chosen D2D pair, and let j iterate over the subcarriers that are not assigned to the chosen D2D pair.

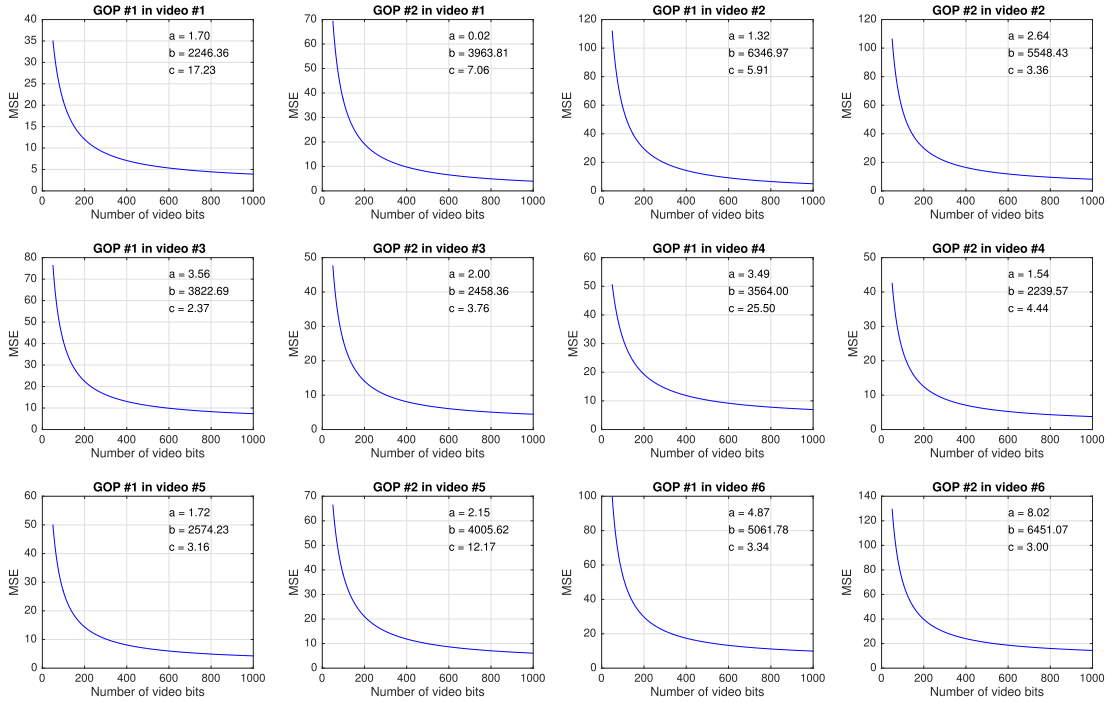

Fig. 6. Rate-distortion curves and parameters of videos.

The chosen D2D pair relinquishes subcarrier i and gains subcarrier j if the total MSE decreases.

- Step 5: Repeat Steps 2 to 4 until all D2D pairs have been considered.

D. PHY-Layer Greedy Assignment and Power Allocation

A greedy subcarrier assignment and power allocation algorithm aiming to maximize the total bit rate of all D2D pairs was proposed in [5]. The subcarrier assignment in [5] was initialized by assigning all D2D pairs to subcarriers in a greedy approach, and did not have any additional steps for local search. As for the power allocation, although the PHY-layer power allocation problem is non-convex [7], local maxima can be found using the bisection search algorithm proposed in [5]. This algorithm was based on orthogonal "subchannels", and details of waveform design were not provided. For the purpose of comparison, we adapt the algorithm from [5] as a baseline by replacing "subchannels" by subcarrier groups. We also remove all constraints related to the cellular users in [5], such as the throughput constraints of cellular users, as our paper aims to investigate resource sharing among D2D pairs in a dedicated spectrum. Also, the objective function used in [5] is based on the capacity of Gaussian channels in AWGN. For a fair comparison over Rayleigh fading channels, the objective function in the baseline algorithm from [5] is replaced by the average number of bits per symbol from (15).

V. Simulation Results and Discussion

We simulate a D2D system with 24 subcarriers, each with 15kHz bandwidth. Each subcarrier uses a raised-cosine pulse with roll-off factor 0.5 for pulse shaping and the symbol rate is 10kHz. The channel response consists of path loss, shadowing and multipath fading. The path loss is $46.8+18.7\log_{10}(d[m])$, and the shadowing follows the log-normal distribution with standard deviation of 3dB [20]. The subcarriers experience independent Rayleigh fading due to multipath, and the channel response is assumed to be flat within a subcarrier. The two-sided noise power spectral density is -174 dBm/Hz. The SER target is 10^{-3} in the simulation. The supported modulation formats are 4-QAM, 16-QAM, 64-QAM and 256-QAM. We consider a single cell whose radius is 1000 meters. D2D transmitters and receivers are uniformly distributed in the cell, and the distance between transmitter and receiver in each D2D pair is restricted between 10 and 50 meters.

We use 6 video sequences with a resolution of 640×480, encoded by H.264/SVC reference software JSVM version 9.19.15. The length of each video sequence is 10 seconds at 30 frames per second, and the video is organized in GOPs of 15 frames (I-P-P-P). The 4×4 DCT coefficients for the MGS layer of each macroblock are split with MGS vector [1, 1, 2, 2, 2, 8] [21]. The parameters of videos and rate-distortion curves are shown in Fig. 6. The video contents are protected by a rate $2/3$ low density parity check code from DVB/C2 [22]. Each packet consists of 300 bytes of FEC plus data bits. The video quality is evaluated by peak signal-to-noise ratio (PSNR), which is defined by $\text{PSNR} \triangleq 10\log_{10}\{255^2/E[\text{MSE}]\}$. For the transmission of the video, the subcarriers are divided into 4 groups, where each group has 6 subcarriers with a total bandwidth 90kHz.

A. Simulation Results for Different Local Search Methods in Subcarrier Assignment

A cell with $K = 40$ D2D pairs is simulated to compare the different methods of local search. The power constraint for each D2D pair is 10 mW. To evaluate the complexity of

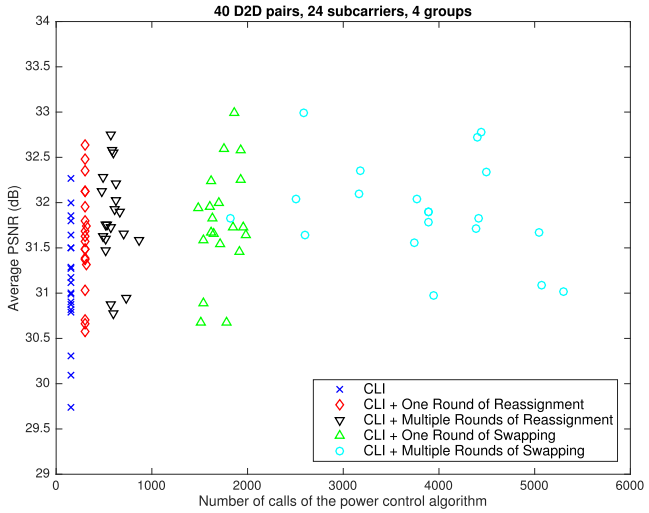

Fig. 7. Tradeoff between complexity and average PSNR for different local search methods. CLI refers to cross-layer initialization.

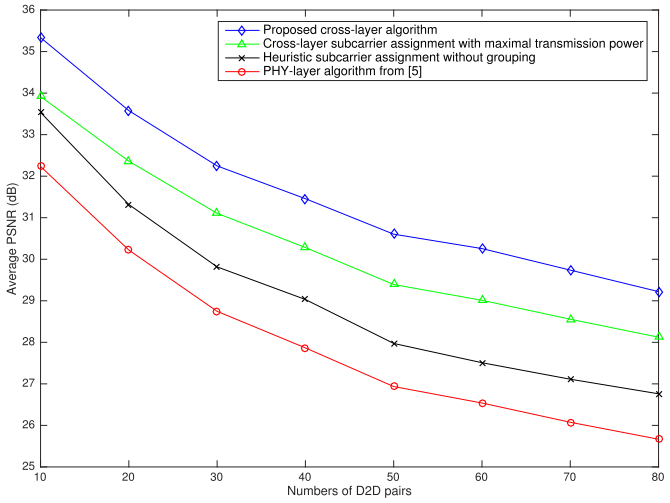

Fig. 9. Average PSNR for the proposed algorithm in comparison with baseline algorithms. The power constraint of each D2D transmitter is 10mW.

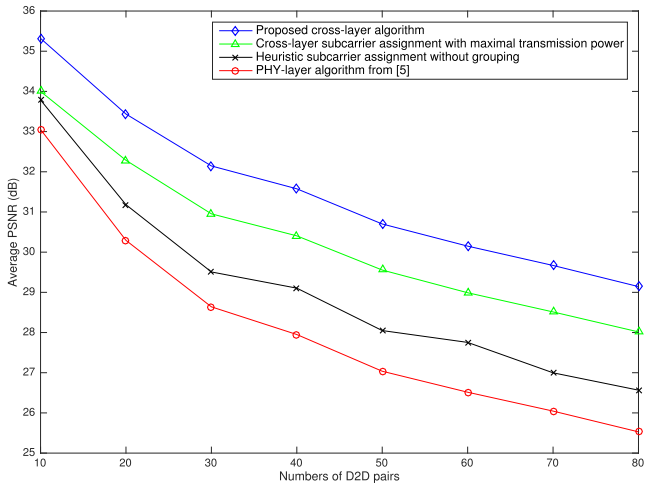

Fig. 8. The average PSNR for the proposed algorithm in comparison with baseline algorithms. The power constraint of each D2D transmitter is 100mW.

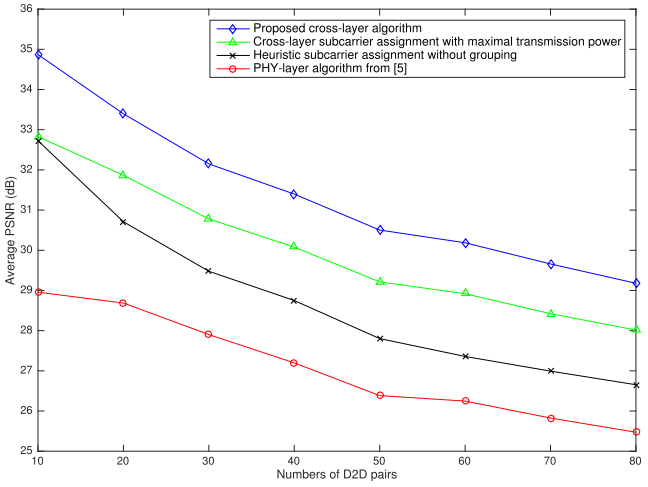

Fig. 10. Average PSNR for the proposed algorithm in comparison with baseline algorithms. The power constraint of each D2D transmitter is 1mW.

different search methods in subcarrier assignment, we simulate 20 realizations of geographical locations, each with independent channels and randomly selected video sequences with random starting points. Under this setting, the tradeoff between the average video PSNR and the complexity of different local search methods can be seen in Fig. 7. The plot shows the number of times that the power allocation algorithm is called, and the corresponding average PSNR in each realization. Cross-layer initialization alone generates acceptable average PSNR, but is still more than 0.8dB inferior in the worst case and more than 0.4dB inferior in the best case than other subcarrier assignment methods. After one round of subcarrier reassignment, the average PSNR is already very close to the local optimum. Running multiple rounds of subcarrier reassignment delivers negligible gains in average PSNR, but almost doubles the complexity. Subcarrier swapping requires a significantly larger computational effort than subcarrier reassignment, but only leads to marginal gains in average PSNR. Based on the results at Fig. 7, we choose cross-layer initialization with a single round of subcarrier assignment in our proposed algorithm.

B. Simulation Results of Proposed Algorithm Compared to Baseline Algorithms

We simulate a cell with $K = 10$ to 80 D2D pairs, and compare the performance of the proposed cross-layer algorithm with baseline algorithms, as shown in Figures 8 - 10. The power constraint for each D2D pair is 100, 10 and 1 mW in Figures 8 - 10, respectively. In Figures 8 - 10, the proposed algorithm outperforms baseline algorithms by more than 1dB in the average PSNR. The cross-layer subcarrier assignment with maximal transmission power has the best average PSNR among the baseline algorithms, but is still more than 1dB inferior to the proposed algorithm, due to the absence of cross-layer power allocation. The average PSNR of the heuristic subcarrier assignment algorithm is approximately 2dB lower than the proposed algorithm. The average PSNR of the

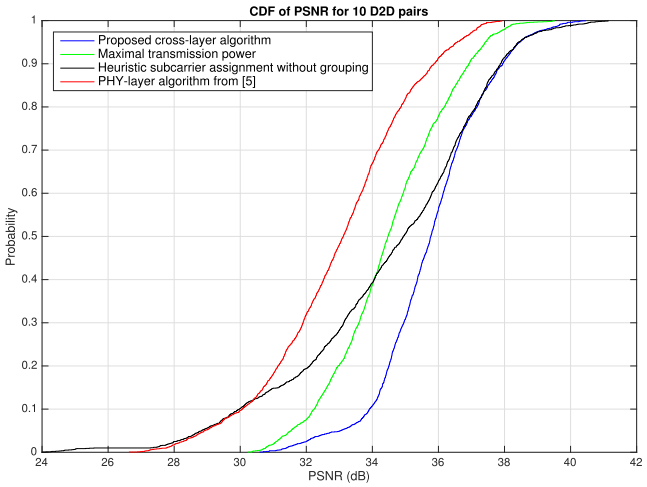

Fig. 11. Distribution of PSNR for the proposed algorithm in comparison with baseline algorithms for $K = 10$ and D2D power constraint 10mW.

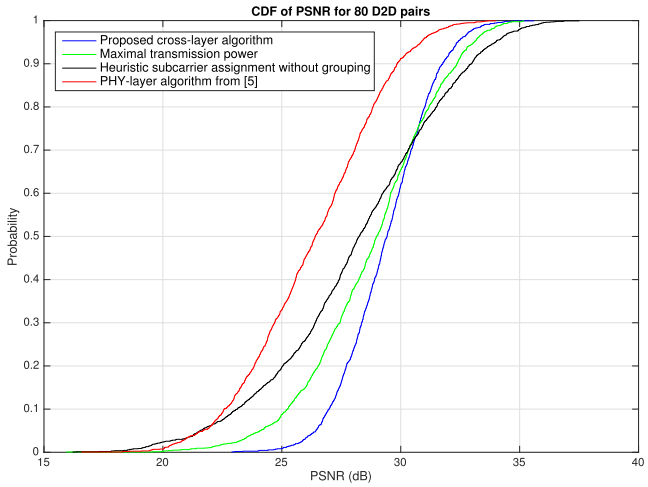

Fig. 12. Distribution of PSNR for the proposed algorithm in comparison with baseline algorithms for $K = 80$ and D2D power constraint 10mW.

TABLE I

OVERALL VIDEO QUALITY AND FAIRNESS COMPARISON FOR D2D POWER CONSTRAINT 10mW

	$K = 10$				$K = 80$			
	Proposed	MaxPower	Heuristic	PHY[5]	Proposed	MaxPower	Heuristic	PHY[5]
Average PSNR (dB)	35.33	33.94	33.58	32.17	29.19	28.08	26.83	25.64
Standard Deviation of PSNR (dB)	1.64	1.76	3.01	2.20	1.87	2.74	3.72	2.81
5 percentile PSNR (dB)	30.51	30.18	24.00	26.41	22.91	17.02	16.26	17.10

PHY-layer algorithm from [5] is more than 2dB lower than the proposed algorithm when the power constraint is 100mW, and the gap in the average PSNR is in the range of 3 to 6dB for the other transmission power configurations. The reason is that the objective of the PHY layer algorithm is to maximize the total bit rate rather than the video quality. When the system is limited by the power constraint, the bit rates of D2D pairs are relatively low, and the D2D pairs operate at the steep part of the RD curves according to (16). In this case, it is critical to take the slope of the video RD into account to achieve better average video quality, but the PHY-layer algorithm does not take the video RD into consideration.

The cumulative distribution functions of PSNR for $K = 10$ and 80 are shown in Figures 11 and 12, respectively. Similar to the observation on average PSNR, the PHY layer algorithm is the most inferior among the baseline algorithms. The distribution of PSNR for the proposed algorithm is least widely spread among all algorithms considered. Compared to the proposed algorithm, the heuristic algorithm has a slightly larger proportion of D2D pairs operating at high PSNR, but it also has considerable larger proportion of D2D pairs suffering from low PSNR, so the average PSNR of the heuristic algorithm is lower than the proposed algorithm. The maximal power algorithm has a slightly wider spread PSNR than the proposed algorithm. For $K = 10$, the PSNR of the maximal power algorithm is strictly lower than the proposed algorithm. For $K = 80$, the PSNR distribution of the maximal power algorithm has a marginally longer tail on the high PSNR region and a considerably longer tail in the low PSNR region, and the average PSNR is thereby still lower compared to the proposed algorithm. We use both the 5 percentile PSNR and the standard deviation of the PSNR as indicators of fairness. As can be seen in Table I, the proposed algorithm outperforms three baseline algorithms in both the overall video quality and fairness, so the fairness of users has not been sacrificed for a better overall performance.

The relationship between the average PSNR and the power constraint for 10 D2D pairs is shown in Fig. 13. As the power constraint increases, the average PSNR will increase at the beginning, and gradually become flat. The proposed algorithm achieves higher average PSNR than the baseline algorithms over the entire range of power constraints simulated. At a low power constraint, e.g., 10^{-5} W, the gap in average PSNR between the proposed algorithm and the baseline algorithms is larger than 5dB. For a large power constraint, such as 10^{-1} W, under which the average PSNR curves for all algorithms become almost flat, the proposed algorithm still outperforms the baseline algorithms by at least 1dB.

The subcarrier assignment problem considered in this paper is a highly non-convex assignment problem. The optimal solution of subcarrier assignment can be found via exhaustive search. Since exhaustive search has a complexity that grows exponentially with the number of D2D pairs, it is prohibitive when the number of D2D pairs is large. For a small number (e.g., from 2 to 6) D2D pairs and 2 subcarrier groups, the average video PSNR of the proposed algorithm is almost identical to exhaustive search, as shown in Fig. 14.

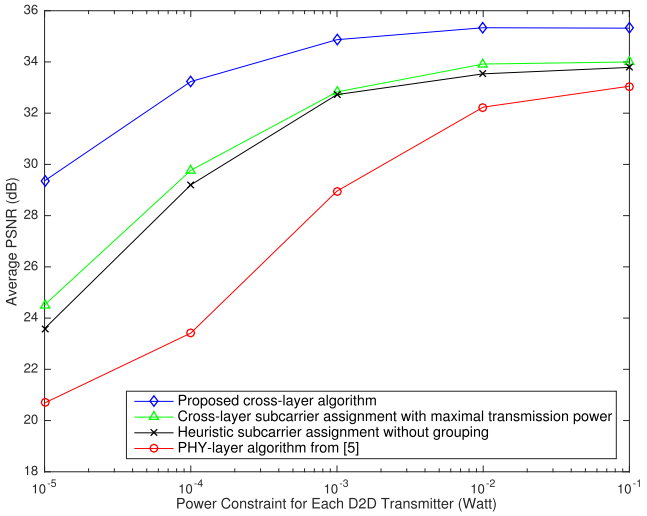

Fig. 13. Average PSNR versus power constraint of each D2D transmitter for $K = 10$ D2D pairs. Power constraint of each D2D transmitter ranges from 10^{-5} W to 10^{-1} W.

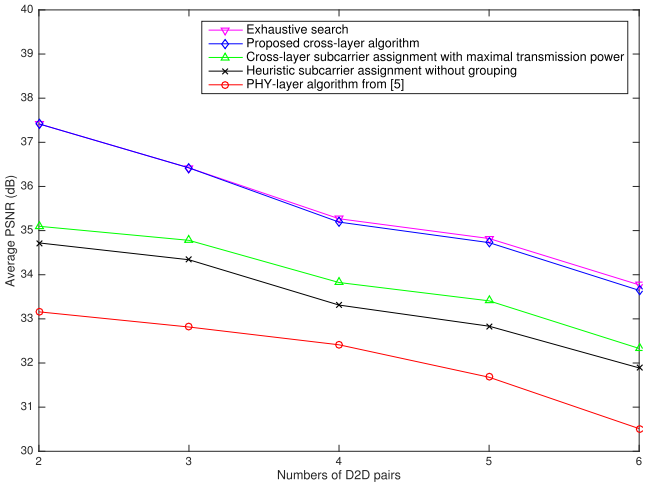

Fig. 14. Average PSNR of exhaustive search algorithm, the proposed algorithm and baseline algorithms for a small number of D2D pairs.

VI. Conclusion

A cross-layer resource allocation algorithm is proposed to optimize the overall quality of D2D video transmission, with an outer loop for subcarrier assignment and an inner loop for power allocation. We derive the condition for the SINR under which the cross layer power allocation problem for D2D video transmission is convex. As a component of the proposed algorithm, the proposed subcarrier assignment scheme achieves a balance between complexity and performance, when compared to other subcarrier assignment schemes in the simulation. Simulation results also demonstrate a considerable improvement by the proposed cross-layer algorithm over baseline algorithms, including an algorithm that uses only physical layer information.

Appendix
Proof of Proposition 1

We show the convexity of $1/[f(e^{-s})+c]$ in s by deriving its second derivative. Let

$$y \triangleq e^{-s}, \tag{32}$$

where $y > 0$, so that $dy/ds = -y$ and $d^2y/ds^2 = y$. Since $f(y)$ is monotonically decreasing in y, $f'(y) < 0$. From (14), the first derivative of $f(y)$ with respect to y is given by

$$\begin{aligned} f'(y) &= \log_2(e)\,\frac{d}{dy}[e^y]E_1(y) + \log_2(e)\,e^y\frac{d}{dy}[E_1(y)] \\ &= f(y) - \log_2(e)\,\frac{1}{y}, \end{aligned} \tag{33}$$

since $\frac{d}{dy}E_1(y) = -e^{-y}/y$. The second derivative of $f(y)$ with respect to y is given by

$$f''(y) = f'(y) + \log_2(e)\,\frac{1}{y^2} = f(y) + \log_2(e)\,\frac{1-y}{y^2}. \tag{34}$$

Ignoring the constant terms, the first and second derivatives of the objective function with respect to y are given by

$$\frac{d}{dy}\left\{\frac{1}{f(y)+c}\right\} = -\frac{f'(y)}{[f(y)+c]^2} \tag{35}$$

and

$$\begin{aligned} \frac{d^2}{dy^2}\left\{\frac{1}{f(y)+c}\right\} &= -\frac{d}{dy}\left[\frac{f'(y)}{[f(y)+c]^2}\right] \\ &= \frac{2[f'(y)]^2 - f''(y)[f(y)+c]}{[f(y)+c]^3}. \end{aligned} \tag{36}$$

Therefore, the second derivative of the objective function with respect to s is given by

$$\begin{aligned} &\frac{d^2}{ds^2}\left\{\frac{1}{f(y)+c}\right\} \\ &= \frac{d^2y}{ds^2}\cdot\frac{d}{dy}\left\{\frac{1}{f(y)+c}\right\} + \left(\frac{dy}{ds}\right)^2\cdot\frac{d^2}{dy^2}\left\{\frac{1}{f(y)+c}\right\} \\ &= -y\cdot\frac{f'(y)}{[f(y)+c]^2} + y^2\cdot\frac{2[f'(y)]^2 - f''(y)[f(y)+c]}{[f(y)+c]^3}. \end{aligned} \tag{37}$$

Thus, $1/[f(e^{-s})+c]$ is convex in s if and only if

$$\frac{d^2}{ds^2}\left\{\frac{1}{f(y)+c}\right\} > 0, \tag{38}$$

which is equivalent to

$$2y[f'(y)]^2 > [f(y)+c]\cdot[f'(y) + yf''(y)] \tag{39}$$

according to (37). We can rewrite (39) using (33) and (34) as

$$\begin{aligned} &2y\left[f(y) - \log_2(e)\,\frac{1}{y}\right]^2 > [f(y)+c] \\ &\cdot\left[f(y) - \log_2(e)\,\frac{1}{y} + y\left(f(y) + \log_2(e)\,\frac{1-y}{y^2}\right)\right]. \end{aligned} \tag{40}$$

For simplicity, let

$$u \triangleq f(y)/\log_2(e) = \ln(2)f(y) = e^y E_1(y), \tag{41}$$

where $f(y) > 0$ according to (14) and the last equality is from (14). Also, we let

$$\tilde{c} \triangleq c/\log_2(e) = c\ln(2). \tag{42}$$

With (41) and (42), we can rewrite (40) as

$$2y\left(u-\frac{1}{y}\right)^2 > (u+\tilde{c})\cdot\left[u-\frac{1}{y}+y\left(u+\frac{1-y}{y^2}\right)\right], \quad (43)$$

which is equivalent to

$$h(u,\tilde{c}) \triangleq y(y-1)u^2-[3+(y+1)\tilde{c}]yu+\tilde{c}y+2>0. \quad (44)$$

For $y \neq 1$, $h(u,\tilde{c})$ is a quadratic function in u, whose discriminant is given by

$$\begin{aligned}\Delta &= [3+(y+1)\tilde{c}]^2y^2-4y(y-1)(\tilde{c}y+2)\\ &= y(\tilde{c}^2y^3+\tilde{c}^2y+y+2\tilde{c}y^2+10\tilde{c}y+2\tilde{c}^2y^2+8). \quad (45)\end{aligned}$$

Since $y>0$ and $\tilde{c}>0$, the discriminant $\Delta>0$.

The roots of $h(u,\tilde{c})=0$ in u are given by

$$u_1=\frac{[(y+1)\tilde{c}+3]y-\sqrt{\Delta}}{2y(y-1)}, \quad u_2=\frac{[(y+1)\tilde{c}+3]y+\sqrt{\Delta}}{2y(y-1)}, \quad (46)$$

where u_1 and u_2 are both functions of y.

From (44), $h(u,\tilde{c})$ can be written as $h(u,\tilde{c}) = Au^2 + Bu + C$, where $A \triangleq y(y-1)$, $B \triangleq -[(y+1)\tilde{c}+3]y$ and $C \triangleq \tilde{c}y+2$. Since $u = e^yE_1(y) > 0$, we are interested in the range of u which satisfies not only $h(u,\tilde{c})>0$ but also $u>0$. Therefore, the range of u where $h(u,\tilde{c})>0,\ u>0$ is given as follows:

1) If $y>1$, then $A>0$, $B<0$ and $C>0$, so $u_1+u_2=-B/A>0$ and $u_1u_2=C/A>0$ [23, pp. 17, 3.8.1]. Therefore, u_1 and u_2 are positive. Since $0<u_1<u_2$ in this case, the range of u where $h(u,\tilde{c})>0,\ u>0$ is $\{u|0<u<u_1 \text{ or } u>u_2\}$;
2) If $0<y<1$, then $A<0$ and $C>0$, so $u_1u_2=C/A<0$ [23, pp. 17, 3.8.1]. Therefore, u_1 and u_2 have different signs. Since $u_1>u_2$ for $0<y<1$, then $u_1>0>u_2$ in this case. Therefore, the range of u where $h(u,\tilde{c})>0,\ u>0$ is $\{u|0<u<u_1\}$;
3) If $y=1$, $h(u,\tilde{c})>0$ simplifies to $u<(\tilde{c}+2)/(2\tilde{c}+3)$. We can show that $\lim_{y\to1}u_1=(\tilde{c}+2)/(2\tilde{c}+3)$, so when $y=1$, the range of u where $h(u,\tilde{c})>0,\ u>0$ is $\{u|0<u<u_1\}$.

Therefore, the solution set of u for $h(u,\tilde{c})>0,\ u>0$ is $\{u|0<u<u_1\}\cup\{u|y>1, u>u_2\}$.

The next step is to convert the solution set of u to the solution set of y, using the fact that u, u_1 and u_2 are functions of y. In fact, from [23, pp. 229, 5.1.19], the following inequality holds for $y>0$:

$$u=e^yE_1(y)\le\frac{1}{y}. \quad (47)$$

Also, the following inequality holds for $y>1$:

$$u_2=\frac{[(y+1)\tilde{c}+3]y+\sqrt{\Delta}}{2y(y-1)}>\frac{3y}{2y(y-1)}>\frac{3(y-1)}{2y(y-1)}>\frac{1}{y}. \quad (48)$$

Combining (47) and (48), $u<u_2$ always holds $\forall y>1$, so $\{u|y>1, u>u_2\}=\varnothing$. Consequently, the range of u where $h(u,\tilde{c})>0,\ u>0$ equals

$$\begin{aligned}&\{u|h(u,\tilde{c})>0,\ u>0\}\\ &=\{u|0<u<u_1,\ y>1\}\cup\{u|u>u_2,\ y>1\}\\ &\cup\{u|0<u<u_1,\ 0<y<1\}\cup\{u|0<u<u_1,\ y=1\}\\ &=\{u|0<u<u_1,\ y>0\}. \quad (49)\end{aligned}$$

Let y^* be the smallest root of $u(y)=u_1(y)$ in $y>0$. From $u \triangleq e^yE_1(y)$ and (46), y^* is equivalently the smallest root of

$$e^yE_1(y)=\frac{[(y+1)c\ln(2)+3]y-\sqrt{\Delta}}{2y(y-1)} \quad (50)$$

in $y>0$. Such a root y^* always exists for the following reasons:

1) $u<u_1$ for $y\to0^+$, where $y\to0^+$ means that y approaches 0 from above. On the one hand, $e^yE_1(y)\le\ln(1+1/y)$ from [23, pp. 229, 5.1.20] and $u=e^yE_1(y)$. By letting $z\triangleq\ln(1+1/y)$, we have

$$\begin{aligned}\lim_{y\to0^+}(\sqrt{y}u) &\le \lim_{y\to0^+}\left[\sqrt{y}\ln\left(1+\frac{1}{y}\right)\right]\\ &= \lim_{z\to+\infty}\frac{z}{\sqrt{e^z-1}}=0 \quad (51)\end{aligned}$$

On the other hand, $\lim_{y\to0^+}\sqrt{y}u_1=\sqrt{2}$ by substituting (45) into (46):

$$\begin{aligned}&\lim_{y\to0^+}(\sqrt{y}u_1)\\ &=\lim_{y\to0^+}\sqrt{y}\cdot\frac{\tilde{c}y^2+(\tilde{c}+3)y}{2y(-1)}\\ &\quad-\lim_{y\to0^+}\sqrt{y}\cdot\frac{-\sqrt{y[\tilde{c}^2y^3+2(\tilde{c}+\tilde{c}^2)y^2+10\tilde{c}y+\tilde{c}^2y+y+8]}}{2y(-1)}\\ &=\sqrt{2}, \quad (52)\end{aligned}$$

Therefore, $\sqrt{y}u<\sqrt{y}u_1$ for $y\to0^+$, and thereby $u<u_1$ for $y\to0^+$.

2) For $y\to+\infty$, $u>u_1$. On the one hand, from [23, pp. 229, 5.1.19], $u=e^yE_1(y)>1/(y+1)$. Therefore, for $y\to+\infty$, u is bounded by

$$u>\frac{1}{y+1}=\frac{y-1}{y^2-1}>\frac{y-1}{y^2}. \quad (53)$$

On the other hand, for $y\to+\infty$, substituting (45) into (46), u_1 is given by

$$\begin{aligned}u_1&=\frac{\tilde{c}y^2+(\tilde{c}+3)y-\sqrt{y^2(\tilde{c}y+1+\tilde{c})^2+8y(\tilde{c}y+1)}}{2y(y-1)}\\ &=\frac{\tilde{c}y^2+(\tilde{c}+3)y-y(\tilde{c}y+1+\tilde{c})\sqrt{1+\frac{8y(\tilde{c}y+1)}{y^2(\tilde{c}y+1+\tilde{c})^2}}}{2y(y-1)}. \quad (54)\end{aligned}$$

Because $[8y(\tilde{c}y+1)]/[y^2(\tilde{c}y+1+\tilde{c})^2] \ll 1$, for $y \to +\infty$, we further have

$$\begin{aligned} u_1 &\approx \frac{\tilde{c}y^2+(\tilde{c}+3)y-y(\tilde{c}y+1+\tilde{c})\left[1+\frac{1}{2}\cdot\frac{8(\tilde{c}y+1)}{y(\tilde{c}y+1+\tilde{c})^2}\right]}{2y^2} \\ &= \frac{\tilde{c}y^2+(\tilde{c}+3)y-y(\tilde{c}y+1+\tilde{c})-\frac{4(\tilde{c}y+1)}{\tilde{c}y+1+\tilde{c}}}{2y^2} \\ &\approx \frac{2y-4}{2y^2}. \end{aligned} \tag{55}$$

Combining (53) and (55), we have $u > u_1$ for $y \to \infty$.

Because $u > u_1$ for $y \to +\infty$ and $u < u_1$ for $y \to 0^+$, there must exist a $y^* > 0$ such that $u(y^*) = u_1(y^*)$, and $u(y) < u_1(y)$ for any y satisfying $0 < y < y^*$. Since c is the only variable besides y in (50), y^* is only dependent on c. From (41), $u(y) = \ln(2) f(y)$, where $f(y) > 0$ is defined in (14), so $0 < u(y) < u_1(y)$ for any y satisfying $0 < y < y^*$. Denoting $s^* \triangleq -\ln(y^*)$, and recalling that $y \triangleq e^{-s}$ from (32), $0 < y < y^*$ is equivalent to $s > s^*$. Therefore, for any s satisfying $s > s^*$, the range of u satisfies $0 < u(y) < u_1(y)$ and $y > 0$, where $y > 0$ is guaranteed by its definition in (32) and always holds.

From (49), the range of u such that $y > 0$, $0 < u(y) < u_1(y)$ holds is equivalent to the range of u such that $h(u(y), \tilde{c}) > 0$, $u(y) > 0$ holds, where $u(y) > 0$ is guaranteed by (41) and always holds. According to (38) - (40), (43) and (44), $h(u(y), \tilde{c}) > 0$ is equivalent to the second derivative of $1/[f(e^{-s}) + c]$ with respect to s being positive, which is equivalent to $1/[f(e^{-s}) + c]$ being convex in s. Therefore, $1/[f(e^{-s}) + c]$ is convex in s over $s > s^*$.

REFERENCES

[1] K. Doppler, M. Rinne, C. Wijting, C. B. Ribeiro, and K. Hugl, "Device-to-device communication as an underlay to LTE-advanced networks," *IEEE Commun. Mag.*, vol. 47, no. 12, pp. 42–49, Dec. 2009.

[2] C.-H. Yu, K. Doppler, C. B. Ribeiro, and O. Tirkkonen, "Resource sharing optimization for device-to-device communication underlaying cellular networks," *IEEE Trans. Wireless Commun.*, vol. 10, no. 8, pp. 2752–2763, Aug. 2011.

[3] G. Yu, L. Xu, D. Feng, R. Yin, G. Y. Li, and Y. Jiang, "Joint mode selection and resource allocation for device-to-device communications," *IEEE Trans. Commun.*, vol. 62, no. 11, pp. 3814–3824, Nov. 2014.

[4] R. Wang, J. Zhang, S. H. Song, and K. B. Letaief, "QoS-aware channel assignment for weighted sum-rate maximization in D2D communications," in *Proc. IEEE Global Commun. Conf. (GLOBECOM)*, Dec. 2015, pp. 1–6.

[5] W. Zhao and S. Wang, "Resource sharing scheme for device-to-device communication underlaying cellular networks," *IEEE Trans. Commun.*, vol. 63, no. 12, pp. 4838–4848, Dec. 2015.

[6] T. Peng, Q. Lu, H. Wang, S. Xu, and W. Wang, "Interference avoidance mechanisms in the hybrid cellular and device-to-device systems," in *Proc. IEEE 20th Int. Symp. Pers., Indoor Mobile Radio Commun.*, Sep. 2009, pp. 617–621.

[7] W. Yu and R. Lui, "Dual methods for nonconvex spectrum optimization of multicarrier systems," *IEEE Trans. Commun.*, vol. 54, no. 7, pp. 1310–1322, Jul. 2006.

[8] Z.-Q. Luo and S. Zhang, "Dynamic spectrum management: Complexity and duality," *IEEE J. Sel. Topics Signal Process.*, vol. 2, no. 1, pp. 57–73, Feb. 2008.

[9] D. Wang, L. Toni, P. C. Cosman, and L. B. Milstein, "Uplink resource management for multiuser OFDM video transmission systems: Analysis and algorithm design," *IEEE Trans. Commun.*, vol. 61, no. 5, pp. 2060–2073, May 2013.

[10] D. Wu, J. Wang, R. Q. Hu, Y. Cai, and L. Zhou, "Energy-efficient resource sharing for mobile device-to-device multimedia communications," *IEEE Trans. Veh. Technol.*, vol. 63, no. 5, pp. 2093–2103, Jun. 2014.

[11] Q. Wang, W. Wang, S. Jin, H. Zhu, and N. T. Zhang, "Quality-optimized joint source selection and power control for wireless multimedia D2D communication using Stackelberg game," *IEEE Trans. Veh. Technol.*, vol. 64, no. 8, pp. 3755–3769, Aug. 2015.

[12] P. Wu, P. C. Cosman, and L. B. Milstein, "Resource allocation for multicarrier D2D video transmission based on exact symbol error rate," in *Proc. IEEE Global Commun. Conf. (GLOBECOM)*, Dec. 2016, pp. 1–7.

[13] P. Wu, P. C. Cosman, and L. B. Milstein, "Resource allocation for multicarrier device-to-device video transmission: Symbol error rate analysis and algorithm design," *IEEE Trans. Commun.*, to be published.

[14] G. Fodor *et al.*, "Design aspects of network assisted device-to-device communications," *IEEE Commun. Mag.*, vol. 50, no. 3, pp. 170–177, Mar. 2012.

[15] M. S. Alouini and A. J. Goldsmith, "Capacity of Rayleigh fading channels under different adaptive transmission and diversity-combining techniques," *IEEE Trans. Veh. Technol.*, vol. 48, no. 4, pp. 1165–1181, Jul. 1999.

[16] H. Schwarz, D. Marpe, and T. Wiegand, "Overview of the scalable video coding extension of the H.264/AVC standard," *IEEE Trans. Circuits Syst. Video Technol.*, vol. 17, no. 9, pp. 1103–1120, Sep. 2007.

[17] K. Stuhlmuller, N. Farber, M. Link, and B. Girod, "Analysis of video transmission over lossy channels," *IEEE J. Sel. Areas Commun.*, vol. 18, no. 6, pp. 1012–1032, Jun. 2000.

[18] S. Boyd and L. Vandenberghe, *Convex Optimization*. Cambridge, U.K.: Cambridge Univ. Press, 2009.

[19] D. P. Bertsekas, *Nonlinear Programming*. Belmont, MA, USA: Athena scientific, 1999.

[20] C. Xu, L. Song, and Z. Han, *Resource Management for Device-to-Device Underlay Communication*. Berlin, Germany: Springer, 2014.

[21] T. Schierl, T. Stockhammer, and T. Wiegand, "Mobile video transmission using scalable video coding," *IEEE Trans. Circuits Syst. Video Technol.*, vol. 17, no. 9, pp. 1204–1217, Sep. 2007.

[22] *Digital Video Broadcasting (DVB); Frame Structure Channel Coding and Modulation for a Second Generation Digital Transmission System for Cable Systems (DVB-C2)*, ETSI Standard EN 302 769, Rev. 1.3.1, Oct. 2015.

[23] M. Abramowitz *et al.*, *Handbook of Mathematical Functions*. New York, NY, USA: Dover 1972.

Peizhi Wu (S'12) received the B.E. degree in electronic engineering from Tsinghua University, Beijing, China, in 2011, and the M.S. and Ph.D. degrees in electrical engineering from the University of California at San Diego, La Jolla, CA, USA, in 2014 and 2016, respectively. He was with the Wireless Connectivity Group, Broadcom Inc., San Diego, CA, in 2013, and was with the Nokia Research Center, Berkeley, CA, in 2014. He is currently a Senior System Engineer at Qualcomm Inc., San Diego. His research interests are in wireless communications, video transmission, cross-layer design, and interference management.

Pamela C. Cosman (S'88–M'93–SM'00–F'08) received the B.S. degree (Hons.) in electrical engineering from the California Institute of Technology, Pasadena, CA, USA, in 1987, and the Ph.D. degree in electrical engineering from Stanford University, Stanford, CA, in 1993. Following post-doctoral fellowships at Stanford University and the University of Minnesota, in 1995 she joined the faculty of the Department of Electrical and Computer Engineering, University of California at San Diego, CA, and is currently a Professor. She was the Director of the Center for Wireless Communications from 2006 to 2008 and the Associate Dean for Students of the Jacobs School of Engineering from 2013 to 2016. Her research interests are in the areas of image and video compression and processing and wireless communications.

Dr. Cosman has been a member of the technical program committee or the organizing committee for numerous conferences, including ICIP 2008–2011, QOMEX 2010–2012, ICME 2011–2013, VCIP 2010, Packet Video 2007–2013, WPMC 2006, ICISP 2003, ACIVS 2002–2012, and ICC 2012. She was the Technical Program Chair of the 1998 Information Theory Workshop held in San Diego. She was an Associate Editor of the IEEE COMMUNICATIONS LETTERS from 1998 to 2001, the IEEE SIGNAL PROCESSING LETTERS from 2001 to 2005, and the Editor-in-Chief from 2006 to 2009 and a Senior Editor from 2003 to 2005 and from 2010 to 2013 of the IEEE JOURNAL ON SELECTED AREAS IN COMMUNICATIONS.

She is a member of Tau Beta Pi and Sigma Xi. Her awards include the ECE Departmental Graduate Teaching Award, a CAREER Award from the National Science Foundation, a Powell Faculty Fellowship, the Globecom 2008 Best Paper Award, and the HISB 2012 Best Poster Award. For outreach and service work, she has been awarded the 2016 UC San Diego Affirmative Action and Diversity Award and the 2017 Athena Pinnacle Award (Individual in Education).

Laurence B. Milstein (S'66–M'68–SM'77–F'85) received the B.E.E. degree from The City College of New York, NY, USA, in 1964, and the M.S. and Ph.D. degrees in electrical engineering from the Polytechnic Institute of Brooklyn, Brooklyn, NY, in 1966 and 1968, respectively. From 1968 to 1974, he was with the Space and Communications Group, Hughes Aircraft Company, and from 1974 to 1976, he was a member of the Department of Electrical and Systems Engineering, Rensselaer Polytechnic Institute, Troy, NY. Since 1976, he has been with the Department of Electrical and Computer Engineering, University of California at San Diego, La Jolla, CA, USA, where he is currently a Distinguished Professor and the Ericsson Professor of Wireless Communications Access Techniques. He is a former Department Chair of the ECE Department, and works in the area of digital communication theory with special emphasis on spread-spectrum communication systems. He has also been a consultant to both government and industry in the areas of radar and communications.

Dr. Milstein served on the Board of Governors of the IEEE Communications Society and the IEEE Information Theory Society, and was the Vice President for Technical Affairs of the IEEE Communications Society in 1990 and 1991. He is also a former Chair of the IEEE Fellows Selection Committee. He has been an Associate Editor for the Communication Theory of the IEEE TRANSACTIONS ON COMMUNICATIONS, an Associate Editor for book reviews of the IEEE TRANSACTIONS ON INFORMATION THEORY, an Associate Technical Editor of the *IEEE Communications Magazine*, and the Editor-in-Chief of the IEEE JOURNAL ON SELECTED AREAS IN COMMUNICATIONS. He was a recipient of the 1998 Military Communications Conference Long Term Technical Achievement Award, an Academic Senate 1999 UCSD Distinguished Teaching Award, an IEEE Third Millennium Medal in 2000, the 2000 IEEE Communications Society Armstrong Technical Achievement Award, various prize paper awards, including the 2002 Fred Ellersick MILCOM Award, the IEEE Communication Theory Technical Committee Service Award in 2009, the CTTC Technical Achievement Award in 2012, and the UCSD Chancellors Associates Award for Excellence in Graduate Teaching in 2015.